Interaction of a Compressible Fluid and an Elastic Membrane

JOHN C. O'CALLAHAN*
KPA Nuclear Inc., Waltham, Mass.
AND
RICHARD MADDEN†
Bolt Beranek and Newman Inc., Cambridge, Mass.

The paper presents results from a computer method for analyzing the unsteady interaction of a fluid and an initially flat circular elastic membrane. The method consists of an implicit coupling of computer programs for the fluid flowfield and for the membrane. The pressures and velocities in the flowfield are determined from a scheme based on the method of characteristics in three independent variables. The membrane is represented by a discrete number of points which are tracked as a function of time; lines connecting these points separate the fluid field into noninteracting regions. Deflected membrane shapes, pressure profiles, and the flowfield at various times are presented. The maximum deflection from the coupled analysis is shown to be only 60% of that obtained when the pressure on the membrane is maintained at the pressure associated with stagnating the freestream.

Nomenclature

C_p = pressure coefficient
c = isentropic sound speed
E = function of entropy
h = time step
h_r = spacing between points on membrane
M = Mach number
N = tension per unit length of membrane
P = pressure
P_s = stagnation pressure of freestream
R = membrane radius
r = radial coordinate
s = entropy
t = time
U = radial velocity
$\bar{U}$ = velocity normal to membrane
V = axial velocity
$\bar{V}$ = velocity tangential to membrane
W = membrane deflection
W_s = static deflection of membrane under pressure P_s
z = axial coordinate
α = angle between r and ξ axes
β_i = $\frac{1}{2}(\psi_0 + \psi_i)$
γ = ratio of specific heats
ΔP = pressure difference across membrane
η = tangential coordinate to membrane
θ = angle between projection of inward normal to bicharacteristic on r,z plane and r axis
$\bar{\theta}$ = $\theta - \alpha$
ξ = normal coordinate to membrane
ρ = fluid density
ρ^* = surface density of membrane
σ = $P^{(\gamma-1)/(2\gamma)}$
ψ = $[(2/(\gamma - 1)](\gamma E^{1/\gamma})^{1/2}$

Subscripts

f = fluid
i = ith bicharacteristic
m = membrane
0 = updated time-plane
p = particle path
∞ = freestream

Presented as Paper 70-75 at the AIAA 8th Aerospace Sciences Meeting, New York, January 19–21, 1970; submitted February 13, 1970; revision received September 30, 1970. Research performed while the authors were at Northeastern University, Boston, Massachusetts, and was supported by NASA Grant NGR-22011042.

* Technical Director. Member AIAA.
† Senior Engineering Scientist. Member AIAA.

I. Introduction

ONE of the major deficiencies in assessing proposed parachute configurations and extended capabilities of existing configurations is the lack of a prediction scheme for the maximum canopy stresses which occur during deployment. The literature contains a number of analyses of stresses in a parachute,[1–4] unfortunately, available analyses are not sufficient to give a complete picture of the stress history. For example, Ref. 1 considers only the time independent stress distribution in a parachute in steady descent. References 2, 3, and 4 attempt to determine a dynamic stress distribution to more closely assess the maximum canopy stress, however, the dynamic analyses also have limitations. For example, the stresses predicted the methods of Ref. 2, as pointed out in Ref. 3, are much too low to account for parachute failures. Reference 3, on the other hand, requires experimental data as input and therefore would be difficult to apply in the assessment of the stresses in a new parachute design. A rigorous development of the equations for stress in a parachute is given in Ref. 4; however, this set of equations requires that the pressure on the canopy be a known function of space and time. It is evident that one great deficiency in even the dynamic analyses is the neglect of the coupling between the flowfield and the canopy. The coupling is so complex that it is not readily amenable to simple modeling and therefore would seem to dictate that one must rely on the use of a digital computer code. The computer method under consideration is a first step in this direction.

The method that is in the development stage will be illustrated through the use of a physically simple example, which although not sufficiently sophisticated to give quantitative results applicable to parachutes, does show the importance of considering the interaction. The example deals with a computer solution of the interaction of a freestream of air and a circular linear membrane. This problem was chosen to illustrate some results from the computer method and to compare these results of the usual uncoupled analysis where the air is assumed to apply a constant pressure to the membrane.

The computer method consists of an implicit coupling of computer programs for the air and the structure. The aero-

dynamic computer program solves the inviscid nonheat conducting unsteady fluid dynamic equations in cylindrical coordinates using an approach based on the method of characteristics. Provisions are included for tracing the motion of the membrane and, consequently, realistic conditions on velocity and pressure may be applied at the fluid membrane interface. The techniques used here are similar to those employed in Refs. 5 and 6. The structure is assumed to be a linear membrane which is solved by finite difference methods. The coupling of the fluid and structure routines has been done in a general manner that allows the substitution of a new structural model by merely changing one subroutine.

II. Governing Equations

The complete model of a fluid interacting with a membrane requires the general governing equations describing the motion of the membrane and the fluid together. Obtaining an exact solution to this set of equations with their associated coupled, time dependent, boundary conditions would be a formidable, if not impossible, task. Therefore, it seems advisable to approach this problem numerically by developing separate computer programs and then coupling them through the boundary conditions; this requires a model for the fluid and a model for the membrane. The models utilized in the present approach are discussed in the following Sections.

Fluid Model

The unsteady inviscid axisymmetric equations are used to model the fluid portion of the interaction. These equations are as follows:

Continuity:

$$D\rho/Dt + \rho(\partial U/\partial r + \partial V/\partial z + U/r) = 0 \qquad (1a)$$

Radial momentum:

$$\rho DU/Dt + \partial P/\partial r = 0 \qquad (1b)$$

Axial momentum:

$$\rho DV/Dt + \partial P/\partial z = 0 \qquad (1c)$$

Conservation of entropy along a particle path:

$$DP/Dt - c^2 D\rho/Dt = 0 \qquad (1d)$$

Perfect gas equation:

$$P = E(s)\rho^\gamma \qquad (1e)$$

where

$$D/Dt = \partial/\partial t + U\partial/\partial r + V\partial/\partial z$$

and ρ is the density, P the pressure, s the entropy, r and U the radial coordinate and velocity, respectively; z and V the axial coordinate and velocity, respectively; t the time, c the isentropic sound speed, and E a function of entropy. Equation (1d) is used to eliminate the ρ derivative in the continuity equation, producing

$$DP/Dt + \rho c^2(\partial U/\partial r + \partial V/\partial z + U/r) = 0 \qquad (2)$$

The application of the method of characteristics to Eqs. (1) and (2) yields two sets of characteristic equations (see, for example, Ref. 6), particle paths that are surfaces of possible discontinuity in the entropy derivative and the usual bicharacteristic equations. Each set is composed of a slope and compatibility equation.

Slope equations along particle paths:

$$dr/dt = U; \quad dz/dt = V \qquad (3)$$

Bicharacteristics:

$$dr/dt = U + c\cos\theta; \quad dz/dt = V + c\sin\theta \qquad (4)$$

where θ is the angle measured between the projection of the inward normal to the bicharacteristic onto the r,z plane and the r axis.

Compatibility equation along particle paths:

Equation (2) may be utilized as a compatibility relationship along a particle path.

Compatibility equation along bicharacteristics:

$$dP/dt + \rho c\cos\theta dU/dt + \rho c\sin\theta dV/dt = -\rho c^2 S \qquad (5)$$

where d/dt represents the total derivative along a bicharacteristic

$$d/dt = D/Dt - c\cos\theta\partial/\partial r + c\sin\theta\partial/\partial z$$

and

$$S = \sin^2\theta\partial U/\partial r - \sin\theta\cos\theta(\partial U/\partial z + \partial V/\partial r) + \cos^2\theta\partial V/\partial z + U/r$$

An alternate form of Eqs. (2) and (5) can be obtained using the perfect gas relation and defining

$$\psi = [2/(\gamma - 1)](\gamma E^{1/\gamma})^{1/2} \text{ and } \sigma = P^{(\gamma-1)/(2\gamma)}$$

The second form of the compatibility equations written in an arbitrary ξ,η coordinate system then becomes

$$\psi d\sigma/dt + c(\partial\bar{U}/\partial\xi + \partial\bar{V}/\partial\eta + U/r) = 0 \qquad (6)$$

$$\psi d\sigma/dt + \cos\bar{\theta}d\bar{U}/dt + \sin\bar{\theta}d\bar{V}/dt = -c\bar{S} \qquad (7)$$

where $\bar{\theta} = \theta - \alpha$ is the characteristic angle measured from the ξ axis, α is the angle between the r and the ξ axis, and $\bar{U}$ and $\bar{V}$ are the velocities in the ξ and η directions, respectively,

$$\bar{S} = \sin^2\bar{\theta}\partial\bar{U}/\partial\xi - \sin\bar{\theta}\cos\bar{\theta}(\partial\bar{U}/\partial\eta + \partial\bar{V}/\partial\xi) + \cos^2\bar{\theta}\partial\bar{V}/\partial\eta + U/r$$

and $\bar{U} = U\cos\alpha + V\sin\alpha$, $\bar{V} = V\cos\alpha - U\sin\alpha$. (Note: The U/r term is unchanged in the transformation of coordinates.)

When a point is in the vicinity of the membrane, it is convenient to choose ξ,η as normal and tangential coordinates to the membrane; for other points, the ξ,η coordinates correspond to the usual r,z (i.e., $\alpha = 0$).

Equations (6) and (7) are used to generate the finite difference equations for the fluid. The boundary conditions on the fluid are that the radial velocity at the axis of symmetry is zero and a fluid particle adjacent to the membrane has a zero normal velocity relative to the membrane. The initial conditions are that the membrane is at rest and the air is moving at freestream velocity with ambient pressure and density.

Membrane Model

The membrane is assumed to be a shallow axisymmetric shell that is restricted to small deflections. The partial differential equation of motion is, then,

$$N[\partial^2 W/\partial r^2 + (1/r)\partial W/\partial r] + \Delta P = \rho^*\partial^2 W/\partial t^2 \qquad (8)$$

where N is the tension per unit length of membrane, W the normal deflection, ρ^* the membrane surface density, and ΔP the pressure difference across the membrane. The boundary conditions on the membrane are that it is fixed at its outer edge and that the slope is zero at the origin. The pressure difference across the membrane is obtained from the fluid dynamic analysis.

III. Finite Difference Equations

Fluid Model

The finite difference equivalents of Eqs. (3, 4, 6, and 7) are as follows:

Slope equations along particle paths:

$$r_p = r_0 - U_p h \tag{9a}$$

$$z_p = z_0 - V_p h \tag{9b}$$

Bicharacteristics:

$$r_i = r_0 - (U_i + c_i \cos\theta_i)h \tag{10a}$$

$$z_i = z_0 - (V_i + c_i \sin\theta_i)h \tag{10b}$$

Compatibility equations along particle paths:

$$\beta_p\sigma_0 + \tfrac{1}{2}c_0 h(\partial\bar{U}/\partial\xi + \partial\bar{V}/\partial\eta + U/r)_0 = K_p \tag{11}$$

where

$$K_p = \beta_p\sigma_p - \tfrac{1}{2}c_p h(\partial\bar{U}/\partial\xi + \partial\bar{V}/\partial\eta + U/r)_p$$

and

$$\beta_p = \tfrac{1}{2}(\psi_0 + \psi_p)$$

Bicharacteristics:

$$\beta_i\sigma_0 + \sin\bar{\theta}_i\bar{V}_0 + \cos\bar{\theta}_i\bar{U}_0 + \tfrac{1}{2}c_0 h[\sin^2\bar{\theta}_i\partial\bar{U}/\partial\xi - \sin\bar{\theta}_i\cos\bar{\theta}_i(\partial\bar{U}/\partial\eta + \partial\bar{V}/\partial\xi) + \cos^2\bar{\theta}_i\partial\bar{V}/\partial\eta + U/r]_0 = K_i \tag{12}$$

where

$$K_i = \beta_i\sigma_i + \cos\bar{\theta}_i\bar{U}_i + \sin\bar{\theta}_i\bar{V}_i - \tfrac{1}{2}c_i h\bar{S}_i$$

$$\bar{S}_i = [\sin^2\bar{\theta}\partial\bar{U}/\partial\xi - \sin\bar{\theta}\cos\bar{\theta}(\partial\bar{U}/\partial\eta + \partial\bar{V}/\partial\xi) + \cos^2\bar{\theta}\partial\bar{V}/\partial\eta + U/r]_i$$

$$\beta_i = \tfrac{1}{2}(\psi_0 + \psi_i),\ c_0 = \tfrac{1}{2}(\gamma - 1)\psi_0\sigma_0$$

In these equations, h is the time step; subscript 0 represents quantities in the updated time-plane at which the solution is desired; subscripts i and p represent values in the back time-plane ($t_0 - h$) on the characteristic conoid and the particle path, respectively.

Equations (9–12) are written in a form that is accurate to the order of the time step squared. Equation (12) may appear at first to be of $0(h^3)$; however, the angle θ is not allowed to vary along the bicharacteristic, and thus the equation is of $0(h^2)$. Additionally, Eqs. (11) and (12) use positions in the back time-plane which have been located accurate only to $0(h^2)$ [see Eqs. (9) and (10)]. Therefore, Eq. (11) is also $0(h^2)$. This scheme yields an explicit solution in contrast to the $0(h^3)$ scheme which is implicit and therefore requires iterations. The computing time for this scheme is consequently much smaller than the pure $0(h^3)$ scheme. The present set of equations does, however, involve information from both time planes and, therefore, may be expected to give better results in areas of high gradients than the usual $0(h^2)$ scheme. It should be noted, however, that the accuracies quoted are for an individual time step. The final solution is reduced by one order after a number of time steps and therefore it is accurate to the order of the time step itself.

In general, Eqs. (11) and (12) contain the seven unknowns, σ_0, $\bar{U}_0$, $\bar{V}_0$, $(\partial\bar{U}/\partial\xi)_0$, $(\partial\bar{V}/\partial\eta)_0$, $(\partial\bar{U}/\partial\eta)_0$, $(\partial\bar{V}/\partial\xi)_0$; however, a proper selection of characteristic angles will eliminate some of the unknown derivatives. Once the required number of characteristics are selected, the equations may be solved for P_0, U_0, V_0 to yield values on a spacial grid superimposed on the flowfield at each increment in time.

Membrane Model

The finite difference equivalent of Eq. (10) may be written as

$$W_{k,j+1} = (N/\rho^*)[1 + 1/2(k-1)](h/h_r)^2 W_{k+1,j} + 2[1 - (N/\rho^*)(h/h_r)^2]W_{k,j} + (N/\rho^*)[1 - 1/2(k-1)] \times (h/h_r)^2 W_{k-1,j} - W_{k,j-1} + \Delta P_{k,j}h^2/\rho^* \qquad (k \neq 1) \tag{13a}$$

$$W_{1,j+1} = 4(N/\rho^*)(h/h_r)^2 W_{2,j} + 2[1 - 2(N/\rho^*)(h/h_r)^2] \times W_{1,j} - W_{1,j-1} + \Delta P_{1,j}h^2/\rho^* \qquad (k = 1) \tag{13b}$$

where k represents the kth nodal point and j represents the jth time plane, h is the time step and h_r is the spacial grid spacing.

The difference operators in Eqs. (13) are written to the order of the grid spacing squared and to the order of the time step squared. Note, however, that similar to the fluid portion the order of error in the timewise direction is reduced by one after a number of time steps.

The local velocities of the membrane are then determined from a backward difference operator applied to the deflections

$$V_{k,j+1} = (3W_{k,j+1} - 4W_{k,j} + W_{k,j-1})/2h \qquad j \geq 0$$

where $V_{k,j}$ is the instantaneous velocity of the kth nodal point at the jth time step.

Initial conditions must be prescribed for both the deflections and velocity on the membrane. The initial condition on velocity is used to define $W_{i,-1}$ for the initial time cycle as follows:

$$\partial W_{i,0}/\partial t = (W_{i,1} - W_{i,-1})/2h \tag{14}$$

A discussion of the topological aspects of the computer method together with the procedures for solving the fluid model equations and the coupling of the fluid and structure models is presented in the following sections.

IV. Topological Aspects

A feature of the present method is that the computer program is able to sense a moving boundary (e.g., the membrane) and, consequently, it is able to divide the fluid flowfield into a number of noninteracting regions. The method consists of approximating the membrane by a number of connected straightline segments whose positions are a function of time. The equation of one of these segments is used to decide on which side of the membrane a particular point lies. In this manner it is possible to insure 1) that all points used in a spacial partial derivative approximation are on the same side of the membrane and 2) that the entire numerical conoid of dependence of a point lies on the same side of the parachute. The technique is similar to that presented in Ref. 6.

V. Solution of Fluid Finite Difference Equations

The finite difference equations are solved at each time plane to yield values of the dependent variables on the membrane and also at points on a rectangular grid superimposed on the flowfield. The solution at various locations in the field requires the consideration of two classes of points: points that lie sufficiently far away from a discontinuity and hence have a full conoid of dependence, and points that lie on or near a discontinuity and therefore have a partial conoid of dependence. The numerical representation of the equations and the procedures for handling these two classes of points are discussed in the following sections.

Points Having a Full Conoid of Dependence

For points having a full conoid of dependence, four bicharacteristics and the particle path are required to approximate the conoid. The values for θ_i are chosen, equally spaced, to be 0, $\pi/2$, π, and $3\pi/2$, as shown on Fig. 1.

The values of θ_i are chosen from stability considerations. The calculation requires the choice of a point (r_0,z_0) at which the solution is desired in the new time plane. The location (r_i,z_i) in the previous time plane of the characteristics which pass through (r_0,z_0) may then be determined from Eqs. (9) and (10). It is possible to find a point (r_i,z_i) for which u_i, v_i, and c_i satisy Eqs. (9) and (10) since values of all dependent variables are specified on the grid and on the discontinuities in the previous time plane. However, the solution of Eqs. (9) and (10) is complicated by the fact that there is no explicit relation tying (r_i,z_i) to (U_i,V_i,c_i) in a given time plane. It is therefore necessary to choose some trial location for a bicharacteristic (r_i,z_i) and use an iterative procedure (such as the Newton-Raphson method) to determine the actual coordinates r_i and z_i. Once the coordinates r_i and z_i are established, linear interpolation is performed between the four surrounding grid points (or discontinuities) in the r,z plane to determine the values for all the required dependent variables at (r_i,z_i).

Substituting these values into the four compatibility equations and the particle path relation and reducing gives equations for P_0, U_0, and V_0. These equations are given in Ref. 5.

Points Having a Partial Conoid of Dependence

Points lying on a discontinuity

Points lying on a discontinuity in this analysis are of two types; points on the axis of symmetry and points on the membrane.

Field points on the axis of symmetry: The solution is accomplished by a reflection technique; that is, the bicharacteristic angles $\theta = 0$ and π are symmetrically placed with respect to the axis (see Fig. 1). Thus, the information obtained for bicharacteristic $\theta = \pi$ is also used for $\theta = 0$, in the pertinent equations. The numerical equations for points on the axis must be modified to account for the fact that on the axis the U/r term becomes

$$(U/r)_{r=0} = \partial U/\partial r$$

Points on the membrane: In this case, the orientation of the membrane controls the portion of the conoid that lies in the appropriate region and the original set of $\theta = 0, \pi/2, \pi$, and $3\pi/2$ are not applicable. A routine has been designed to allow the program to find the bicharacteristic angles that correspond to the boundary. The appropriate bicharacteristics are then $\bar{\theta} = \phi, \phi - \pi/2, -\phi$, and $\pi/2 - \phi$ where ϕ is an angle measured from the normal to the discontinuity as shown in Fig. 2. The angle ϕ is assumed to be two-thirds of the way between the normal and the bicharacteristic angle to the closest discontinuity.

The compatibility relations are modified as follows. Since the points are on an impervious membrane, the relative fluid velocity normal to the membrane will be zero. The pressures and velocities are then evaluated in an inertial reference frame that moves at the velocity of the membrane at the point under consideration. The velocity components of the membrane are known quantities and therefore the velocity of the fluid may be determined by adding the velocity of the membrane to the results. The additional relationships needed are

$$\bar{U} = \bar{U}_f - \bar{U}_m \tag{15}$$

$$\bar{V} = \bar{V}_f - \bar{V}_m \tag{16}$$

where all velocity components are measured in the ξ,η reference; $\bar{U},\bar{V}$ are the velocity components of the fluid relative to the membrane, $\bar{U}_f,\bar{V}_f$ the velocity components of the fluid, and $\bar{U}_m,\bar{V}_m$ the velocity components of the membrane.

Points on the membrane and on the axis of symmetry: The procedure here, basically the same as in the previous section, uses a reflection procedure (see Fig. 2). The reflection technique is used in a similar manner to the field points on the axis, except that two points are now reflected with respect to the membrane normal. Additionally, the U/r term must be modified as follows:

$$(U/r)_{r=0} = \partial \bar{V}/\partial \eta$$

Points lying near a discontinuity

The procedure followed here is similar to that for points lying on a discontinuity except that the velocity normal to the discontinuity does not vanish and consequently one additional characteristic is required. The appropriate angles measured from the local normal to the membrane are $\bar{\theta} = \pi/2, -\pi/2, \pi/4, -\pi/4$, and 0 as shown in Fig. 3. If the point is on the axis the reflection technique is again used.

VI. Coupling of Fluid and Structure Models

The coupling of the computer programs for the fluid field and the membrane is done in an implicit manner. The steps

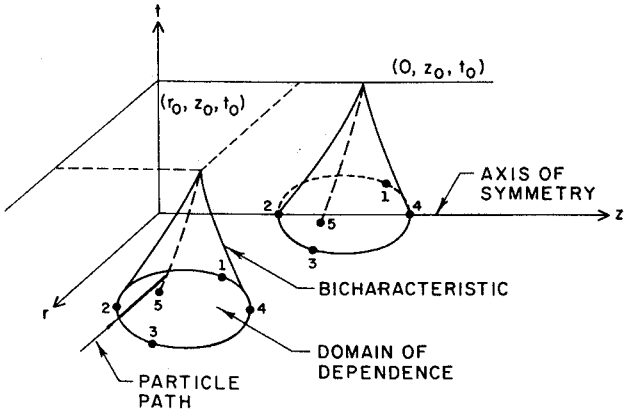

Fig. 1 Flowfield conoids of dependence.

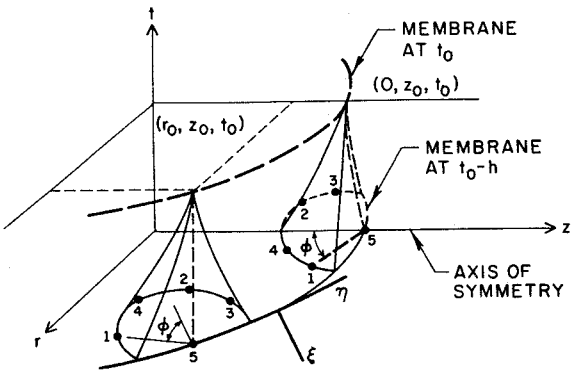

Fig. 2 Partial conoids for points on membrane.

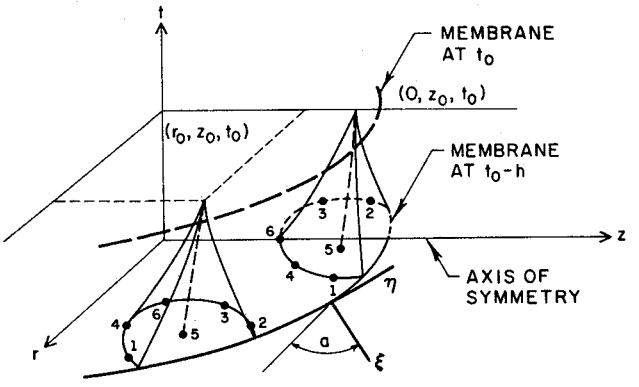

Fig. 3 Partial conoids for points near membrane.

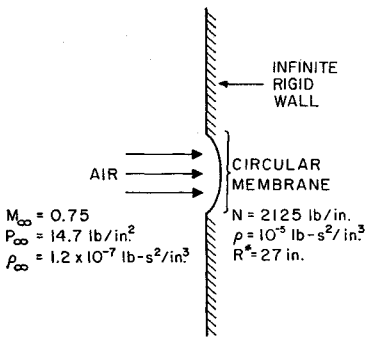

Fig. 4 Membrane configuration.

in the coupling process for a given time-cycle are as follows:

1) The deflection and velocity at each nodal point on the membrane are determined from the pressure differences across the membrane and local velocities on the membrane at the previous two time-steps.

2) The pressures and velocities of the fluid particles adjacent to the membrane are calculated at the positions determined in the previous step.

3) Deflections and velocities on the membrane are again calculated using the average of the pressure at the beginning of the time cycle and the pressure calculated at the updated membrane positions.

4) Step 2 is repeated and a new value for the average pressure during the time step is computed. This average pressure is compared with the average pressure used in step 3. A change in pressure less than or equal to 1% of the average pressure from step 3 is used as a criterion for convergence. If convergence is not established, steps 3 and 4 are repeated until convergence is attained or until a given amount of iterations has been exceeded. Exceeding this limit causes the program to stop.

5) The pressures and velocities are calculated at each point on the rectangular grid that has been superimposed on the flowfield. The maximum number of iterations for steps 3 and 4 has been set as 7; however, with the time step presently used no more than 2 iterations have been required.

VII. Results and Discussion

The case under consideration is the interaction of a uniform freestream of air at a Mach number of 0.75 with a circular membrane bounded by an infinite rigid wall as shown in Fig. 4. The air is assumed to be an ideal gas with $\gamma = 1.4$, a freestream pressure of 14.7 lb/in.^{2} and a freestream density of 1.2×10^{-7} lb-sec^2/in.^{4}. The spacial grid in the flowfield is 3×3 in. and the time step h is 0.75×10^{-5} sec. This time step is approximately 60% of the stability limit as predicted by the Courant, Freidrichs, and Lewy criterion for the freestream. The 54-in.-diam membrane has a mass per unit area of 10^{-5} lb–sec^2/in.^{3} and is subjected to a uniform tension of 2125 lb/in.

As discussed in Ref. 5, the numerical scheme will induce large pressure transients in areas of severe gradients in either pressure or velocity. These transients may be overcome by using a procedure which does not allow numerical diffusion in the vicinity of the large gradient. This will be incorporated into the computer code at a later date; however, for the present, the problem was partially circumvented by using a starting solution. The starting solution assumes that a certain portion of the flowfield is developed upstream of the membrane before the membrane is allowed to move; the large gradients are therefore moved away from the membrane. This does not entirely clear up the problem, but it is effective in eliminating pressure fluctuations on the membrane. Quantitatively, this starting solution assumes that the fluid particles on the membrane and one grid immediately in front of the membrane have the pressure obtained by stagnating the freestream (P_s = 39.75 lb/in.^{2}). The initial velocity of the membrane itself is assumed to be zero. This flowfield corresponds physically to the case where a plug is placed behind the membrane to keep it rigid and then suddenly removed some time after the fluid strikes the plate. For convenience the pressure on the downstream side of the membrane is maintained as ambient throughout the calculation.

Figure 5 presents the ratio of the difference between the pressure on the axis of symmetry of the membrane and P_s divided by P_s. The pressure rise during the initial few computational time-cycles results from numerical diffusion and is nonphysical. The pressure drop which follows is explained by the fact that, as the membrane accelerates in the direction of the freestream, the fluid particles next to the membrane gain in velocity thus reducing their pressure. When the acceleration of the membrane becomes negative, the fluid particles are slowed down and, consequently, the pressure rises again to a peak. The peak occurs just after the maximum deflection of the membrane, the peak pressure being 50% higher than the freestream stagnation pressure. This difference would surely be reflected in an increase in maximum stress if a nonlinear membrane had been considered. As the membrane moves downward, the pressure falls for the next few computational cycles. Following this, there is a dwell in pressure which, as will be shown later with the aid of Figs. 9, 10, and 11, results from the fact that as the membrane pushes fluid back into the flowfield, fluid tends to swirl and form a low fluid velocity zone in front of the membrane. The pressure on the membrane then decreases monotonically in time, with one slight bump, until a minimum is reached. This minimum occurs slightly later than the minimum deflection point. A scale for pressure coefficient C_p is also shown on the plot for reference. The pressure coefficient ranges from 3.2 to 7.2 during the first deflection cycle of the membrane.

Figure 6 presents the pressure ratio across the membrane at various times. The times have been chosen to correspond with (t = 1.1 msec) the minimum pressure on the membrane, (t = 1.88 msec) the maximum pressure on the membrane, and

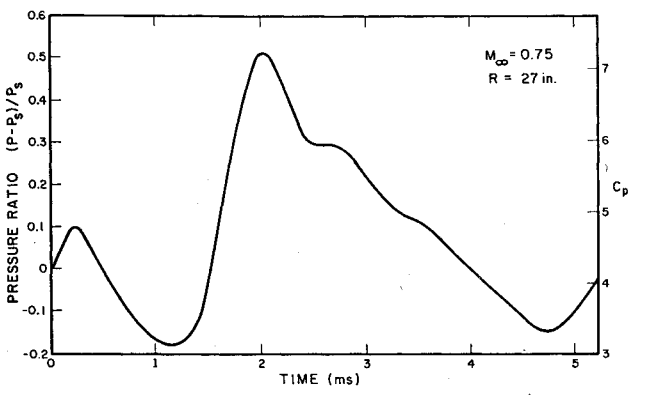

Fig. 5 Pressure at membrane axis of symmetry as a function of time.

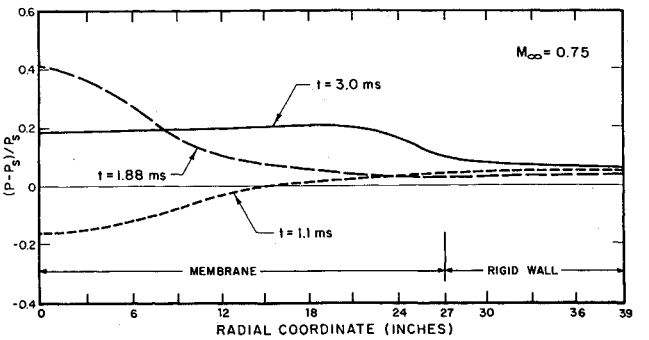

Fig. 6 Pressure distribution on membrane at various times.

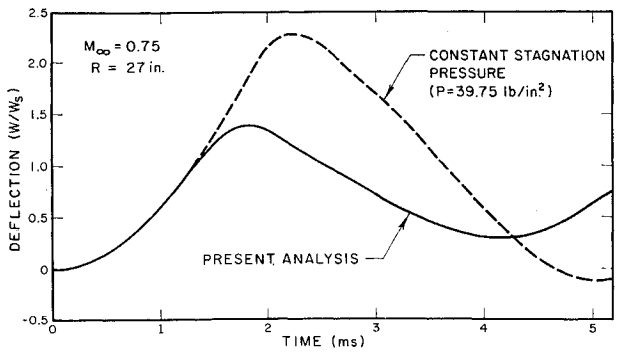

Fig. 7 Membrane deflection at axis of symmetry as a function of time.

(t = 3 msec) a pressure between the maximum and minimum (see Fig. 5). The curves for maximum and minimum pressure illustrate a pressure distribution which is qualitatively similar to the Bessel function dependence required for a pure first mode of vibration of the membrane. On the other hand, the intermediate pressure curve is flat over approximately 80% of the membrane diameter. The change in the spacial distribution of pressure with time precludes the establishment of a loading function on the membrane which is separable in time and radial coordinate. It would then appear that the coupled solution could have considerable advantage over an uncoupled approximation where the loading function must be established a priori as a separable function. All the curves come together just beyond the outer fixed-edge of the membrane at a pressure which is slightly higher than the one-dimensional stagnation pressure (P_s). The pressures on the rigid wall are slightly higher than expected in this example since the computational grid does not extend far enough in the radial direction and, consequently, waves are reflected from it.

In Fig. 7 a comparison is made between deflection results from the present method and those from a solution in which the pressure on the membrane is uniform in space and constant in time at a value P_s = 39.75 lb/in.². The latter case was used to represent typical results from an uncoupled fluid-membrane solution. Figure 7 illustrates the ratio of the dynamic deflection of the membrane point on the axis to the static deflection under a pressure P_s as a function of time. Both curves are similar in shape; however, the interaction case has a smaller maximum deflection which has an earlier time for the occurrence. This is explained by noting that, in the interaction problem, the pressure on the membrane drops below P_s as the membrane accelerates upward. The minimum for the deflection is higher than the constant pressure solution since, as the membrane returns, the pressure is above P_s. It is interesting to note that the frequency of vibration of the membrane as estimated from the half-cycle peak to minimum for the interaction case is 209 Hz which is the fundamental frequency of free vibration of the membrane. (At later times in the solution the mass loading due to the air would be expected to lower this frequency.)

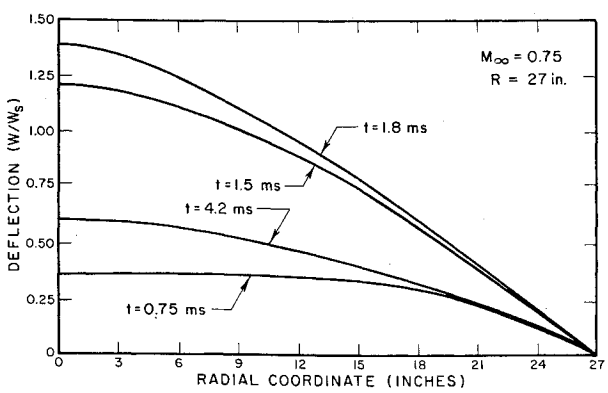

Fig. 8 Deflected membrane shapes at various times.

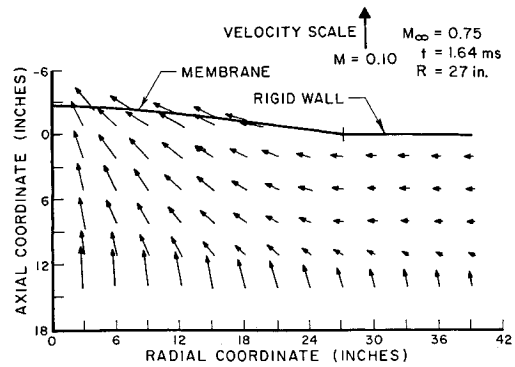

Fig. 9 Velocity field for the fluid below the membrane at t = 1.64 msec.

Figure 8 shows the nondimensional deflected shapes of the membrane at various times. At t = 0.75 msec, the membrane is flat except near the outer edge since the signal that the boundary has zero deflection has not as yet reached the entire membrane. The curves for t = 1.5 and 1.8 msec show an almost first-mode-type shape as the membrane approaches its maximum deflection. The curve for t = 1.8 msec is in fact the maximum deflection. The curve for t = 4.2 msec is approximately at the minimum for the first cycle and is seen to be also in the first mode shape. However, this is no guarantee that the membrane will continue to keep this shape for later cycles. In fact, it appears that there is a tendency during the last few computational cycles for the point on the axis to drop below its neighboring points, thus indicating a contribution of the higher modes of vibration. This should be expected since the loading function contains all modes.

Figures 9, 10, and 11 illustrate the velocity in the fluid flowfield and of fluid particles on the membrane at times t = 1.64, 2.1, and 3.0 msec. Figure 9 shows that, at early times before maximum deflection, the flowfield is directed towards the axis of symmetry as the fluid flows in to fill the additional area created by the deflecting membrane.

Figure 10 illustrates the velocity vectors shortly after the point on the membrane on the axis has reversed direction and the membrane begins to push the fluid back into the free-stream. Note, however, that the outermost points on the membrane are still traveling upwards and that the fluid in this area is traveling towards the axis. The fluid particles pushed back into the field by the membrane encounter forward-moving fluid particles and consequently a swirl is created near the axis. The fluid in this swirl has a low velocity, causing the pressure dwell noted in Fig. 5. Note also that

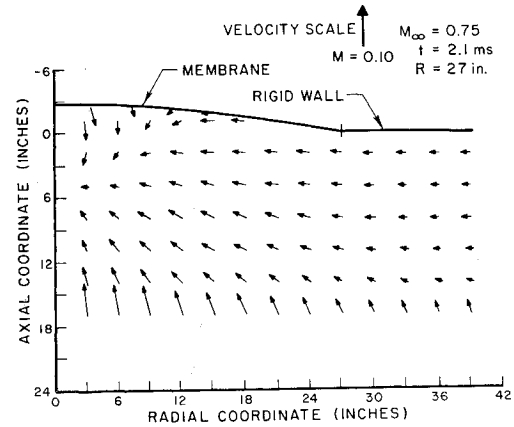

Fig. 10 Velocity field for the fluid below the membrane at t = 2.1 msec.

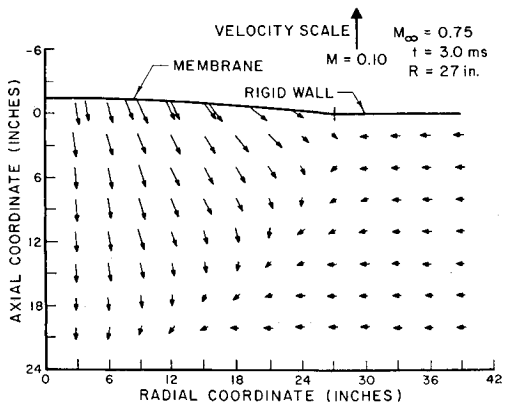

Fig. 11 Velocity field for the fluid below the membrane at $t = 3.0$ msec.

there is a relative stagnation point on the membrane where the inrushing fluid encounters the fluid being pushed out from the axis. The radial velocities near the rigid wall on Figs. 10 and 11 are caused in some measure by the fact that the edge of the computational grid is too close to the edge of the membrane. This problem may easily be fixed, at the expense of additional computer time, by enlarging the computational grid. Figure 11 illustrates a later time when the stagnation point on the membrane has moved out to the edge of the membrane and the entire membrane is now pushing fluid back into the main stream. This behavior is expected to be somewhat typical of future cycles; however, some differences should result due to the contribution of the higher modes of vibration of the membrane and the mass loading effects of the air.

VIII. Concluding Remarks

A numerical method of analysis for determining the interaction of a fluid and a membrane structure has been developed and programed as part of the early stage of development of a computer program for analyzing the stresses in an inflating parachute. The method is based on an analysis of the flowfield using concepts from the numerical method of characteristics coupled implicitly with an analysis of the dynamic response of a linear membrane. The approach is unique in that provisions have been made to recognize boundaries, such as a membrane, in the flowfield, and consequently, physically noninteracting regions may be differentiated and appropriate boundary conditions may be applied on the moving membrane.

The example problem presented illustrates some of the areas in which a coupled aerodynamic/structure solution may differ from an uncoupled solution and, in particular, shows a discrepancy of 50% in maximum pressure and an associated 60% difference in maximum deflection. These differences would surely be reflected in a stress analysis if a nonlinear membrane had been considered.

References

[1] Ross, E. W., Jr., "Approximate Analysis of a Flat Circular Parachute in Steady Descent," 69-51-OSD, Dec. 1968, U.S. Army Natick Labs., Natick, Mass.

[2] Heinrich, H. G. and Jamison, C. R., "Parachute Stress Analysis Inflation and Steady State," *Journal of Aircraft*, Vol. 3, No. 1, Jan. 1966, pp. 52–58.

[3] Asfour, K. J., "Analysis of Dynamic Stress in an Inflating Parachute," *Journal of Aircraft*, Vol. 4, No. 5, Sept.–Oct. 1967, pp. 429–434.

[4] Roberts, B. W., "A Contribution to Parachute Inflation Dynamics," AIAA Paper 68-928, El Centro, Calif., 1968.

[5] O'Callahan, J. C., "An Application of the Method of Characteristics to an Inviscid Fluid Interacting with an Initially Flat Circular Membrane," Ph.D. thesis, Sept. 1969, Dept. of Mechanical Engineering, Northeastern Univ., Boston, Mass.

[6] Madden, R., "Hypervelocity Impact Analysis by the Method of Characteristics," TR-R-298, Jan. 1969, NASA.